Structure Formation - From a Cloud of Atoms to a Crystal -

(T10) Valence electrons in condensed matter:

How interference acts on phase stability and electronic transport

H. Solbrig

1. **Basic aspects**
2. **Electronic properties derived from spectral information**
3. **Spectral curves are formed by electronic interference**
4. **Conclusions**

1. Basic aspects

2. Electronic properties derived from spectral information
3. Spectral curves are formed by electronic interference
4. Conclusions

Effective atoms

electrons −	$\rightarrow$ Coulomb $\leftarrow$	nuclei + they carry the mass $\rightarrow$ gravitation $\leftarrow$

part of the electrons
captured by the nuclei

valence electrons		ions

ions screened
by the valence electrons

valence electrons		effective atoms

conclusion:

- effective atoms modelled by spherical potentials inside of atomic spheres

Atomic sphere with a muffin-tin potential inside

atomic spheres (AS),
space-filling,
slightly overlapping

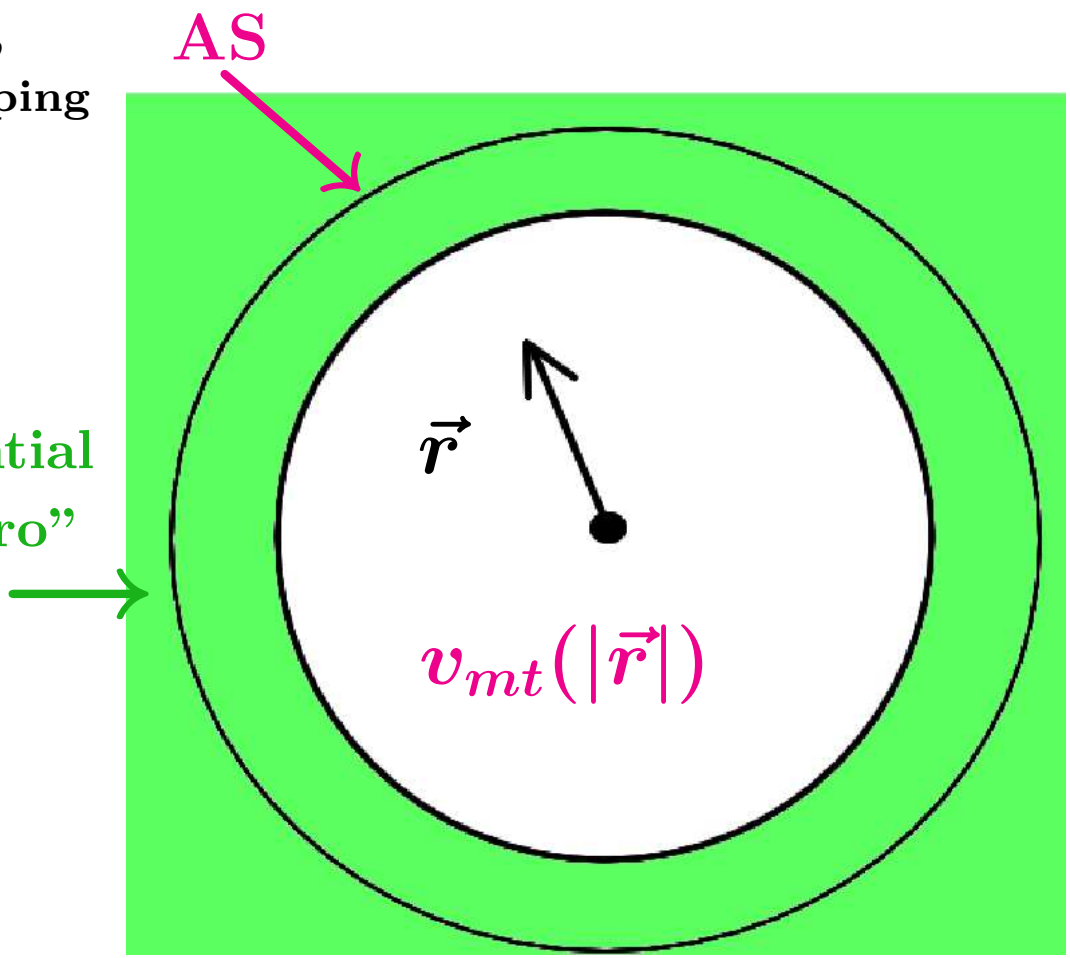

constant potential
"muffin-tin zero"

v_{mt},
spherically symmetric,
no overlap with
adjacent v_{mt}

conclusion:

- effective atoms treated as atomic spheres immersed into a constant potential

Average valence charge density ρ

estimate $\approx$ (atom number density) $\times$ (average number of valence electrons per **free atom**)

1 2 2 2 2 1 2 2 2 2 1 2 3 4 5 6 7

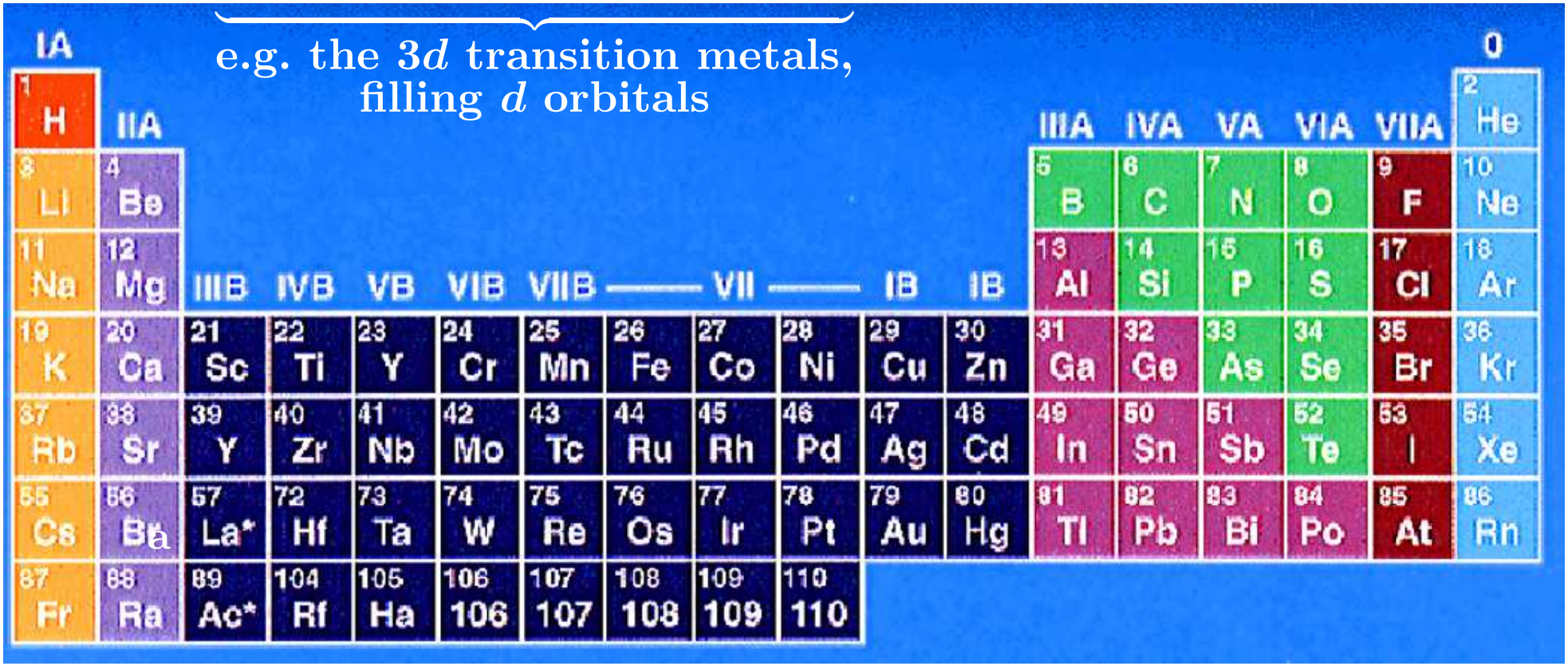

definition:

- **density parameter** r_s = the radius in bohr (a_0) of the average sphere per electron

$$\rho \equiv \left(\frac{4\pi}{3}(r_s a_0)^3\right)^{-1}$$

Real materials have inhomogeneous valence densities

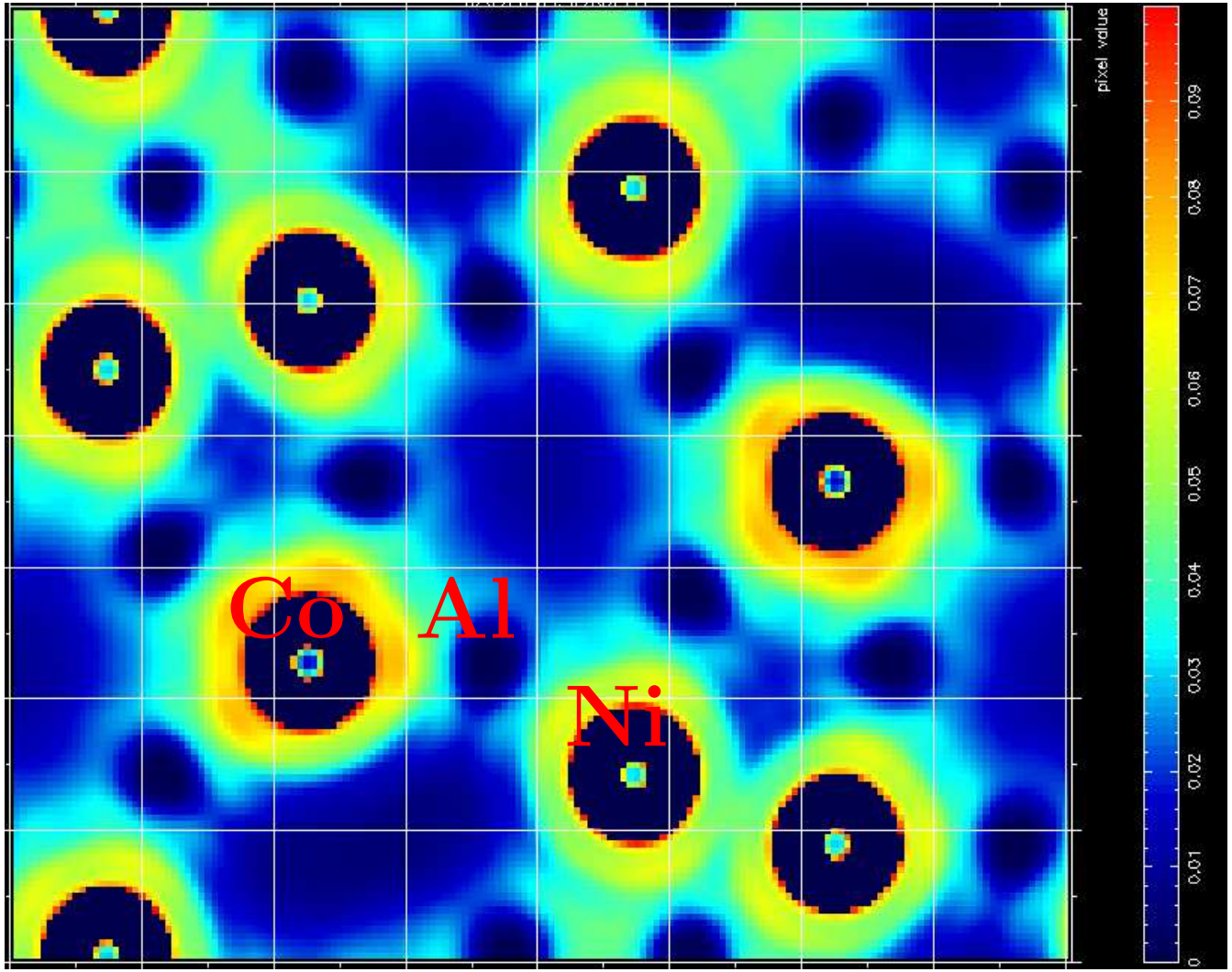

ABINIT & PGPLOT

$Al_{34}Ni_{12}Co_4$
structure model after (Mihalkovič et al. 2002)

average valence density:
$$r_s = 1.6$$

← **cyan**
$r_s \approx 2$ like fcc-Al

conclusion:

- **even trend towards Co - Al covalent bonding**

Scaling with the average valence density: Kinetic energy

scaling relations for the free-electron ground state ($\rho \propto r_s^{-3}$)

$$p_F \propto \rho^{1/3} \propto r_s^{-1}, \qquad \overline{\epsilon_{kin}} \propto \rho^{2/3} \propto r_s^{-2}, \qquad P_{deg} \propto \rho * \overline{\epsilon_{kin}} \propto r_s^{-5}$$

scaling of a small screened Coulomb interaction

$$\overline{\epsilon_C} \propto \rho^{1/3} \propto r_s^{-1}$$

$$\frac{\overline{\epsilon_C}}{\overline{\epsilon_{kin}}} \propto r_s$$

white dwarf stars ($r_s \approx 10^{-2}$) are FE-like with $\sim$ % Coulomb corrections
radius R estimated from pressure equilibrium in the center

$$P_{deg}[\propto R^{-5}] = P_{grav}[\propto R^{-4}]$$

$$\Longrightarrow \; R \approx 7000 \text{ km, just like planets}$$

conclusion:

- increasing electron density makes matter more free-electron like

Scaling with the average valence density: Structure

by increasing external pressure P_{ext} on simple metals

P_{ext}/GPa	low 1	⟹	intermediate a few 10	high 100
structures	bcc fcc		large complex cubic cells	bcc fcc hcp
coordinations	high		lower	high
goals	maximize ion-ion spacings preserves screening		enable Bragg reflections and covalency	avoid overlap of ion cores

by increasing $\frac{\text{electrons}}{\text{atom}}$ ratio on alloying simple metals (watch atom number density)

electrons/atom	1	⟹	1.5	1.8	2
structures		bcc fcc	complex cubic cells	hcp ↑ amorphous most stable	

conclusion:

- increasing valence density promotes the electronic influence

Towards stability at low temperatures

$$\underbrace{\int^{\epsilon_F} d\epsilon\, \epsilon\, \overbrace{n(\epsilon)}^{\text{density of states}}}_{\text{electronic band energy}} + \underbrace{E_{est}}_{\text{electrostatic energy}} \Longrightarrow \text{Min}$$

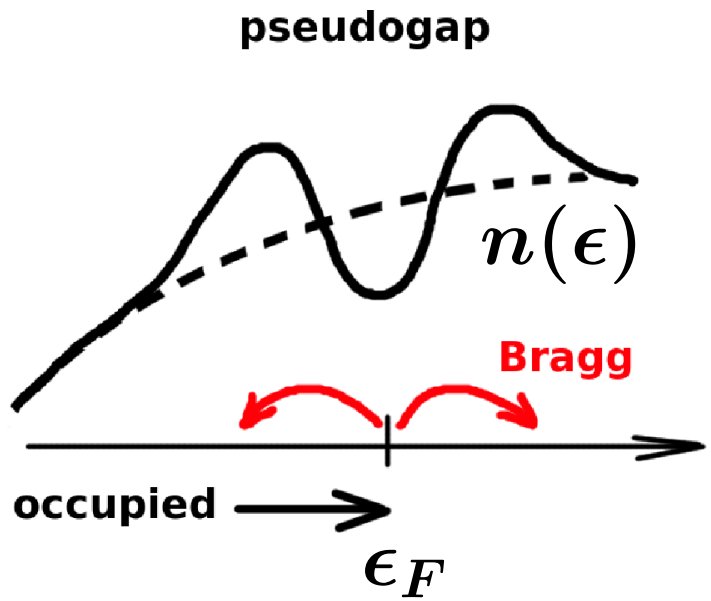

conclusions:

- **avoid** charged effective atoms
- **create** half-occupied pseudogaps at the Fermi energy

1. Basic aspects

2. Electronic properties derived from spectral information

3. Spectral curves are formed by electronic interference
4. Conclusions

Temperature-dependent weighting of spectral information

electronic conductivity $\sigma(T)$

$$\vec{j} = \sigma(T)\,\vec{E}$$
$$\sigma(T) = \mathcal{L}^{11}(T)$$

thermopower $S(T)$ ……

$$\vec{E} = S(T)\,\frac{\partial}{\partial \vec{r}}\,T(\vec{r})$$
$$S(T) = \frac{1}{|e|T}\,\frac{\mathcal{L}^{12}(T)}{\sigma(T)}$$

kinetic coefficients

$$\mathcal{L}^{ij}(T) = \int d\epsilon\,\sigma(\epsilon)\,W^{ij}(\epsilon-\mu(T))$$

$$\mu(T) \approx \epsilon_F - \frac{\pi^2}{6}\left(\frac{d\,ln(n(\epsilon))}{d\,\epsilon}\right)_{\epsilon_F}(k_B T)^2 + \ldots \qquad \text{(chemical potential)}$$

weight functions W^{ij} derived from the Fermi-Dirac distribution $f^0(\epsilon-\mu(T))$

$$W^{11} = -\frac{\partial f^0}{\partial \epsilon}$$

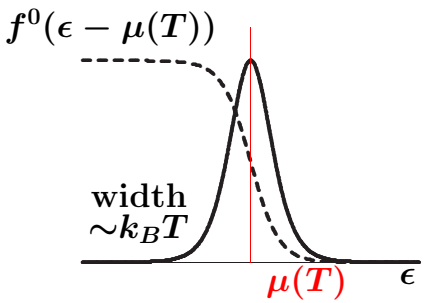

$$W^{12} = -(\epsilon-\mu)\left(-\frac{\partial f^0}{\partial \epsilon}\right)$$

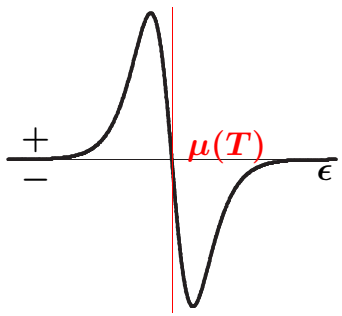

Temperature-dependent weighting of spectral information

electronic conductivity $\sigma(T)$

$$\vec{j} = \sigma(T)\,\vec{E}$$
$$\sigma(T) = \mathcal{L}^{11}(T)$$

thermopower $S(T)$ ……

$$\vec{E} = S(T)\,\frac{\partial}{\partial \vec{r}}\,T(\vec{r})$$
$$S(T) = \frac{1}{|e|T}\,\frac{\mathcal{L}^{12}(T)}{\sigma(T)}$$

kinetic coefficients

$$\mathcal{L}^{ij}(T) = \int d\epsilon\,\sigma(\epsilon)\,W^{ij}(\epsilon-\mu(T))$$

$$\mu(T) \approx \epsilon_F - \frac{\pi^2}{6}\left(\frac{d\,ln(n(\epsilon))}{d\epsilon}\right)_{\epsilon_F}(k_B T)^2 + \ldots \qquad \text{(chemical potential)}$$

weight functions W^{ij} derived from the Fermi-Dirac distribution $f^0(\epsilon-\mu(T))$

$$W^{11} = -\frac{\partial f^0}{\partial \epsilon}$$

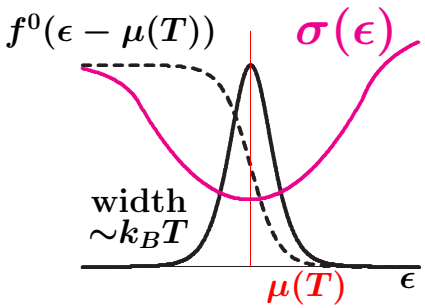

$$W^{12} = -(\epsilon-\mu)\left(-\frac{\partial f^0}{\partial \epsilon}\right)$$

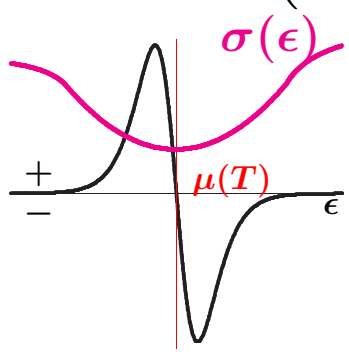

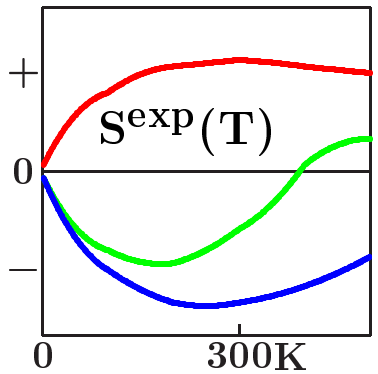

conclusion:

- peculiar temperature dependence due to spectral fine structures on the thermal scale

Spectral information calculated by the LMTO method

unit cell $\longrightarrow$ **Linear Muffin-Tin Orbital method** [1)] $\xrightarrow{\eta_l}$ **for analyzing within the scattering theory**

$|\alpha\rangle$, ϵ_α $\swarrow$ $\qquad$ ϵ_α $\searrow$

conductivity [2)]

$$\sigma(\epsilon) = \frac{e^2 h}{V} \langle \sum_{\alpha,\beta} |\langle\alpha|v|\beta\rangle|^2 \delta(\epsilon - \epsilon_\alpha)\delta(\epsilon - \epsilon_\beta)\rangle_{\vec{k}}$$

density of states

$$n(\epsilon) = \langle \sum_{\alpha} \delta(\epsilon - \epsilon_\alpha)\rangle_{\vec{k}}$$

$\searrow$ $\qquad$ $\swarrow$

diffusivity [3)]

$$\sigma(\epsilon) = \frac{e^2}{V} n(\epsilon) D(\epsilon)$$

1) O.K. Andersen 1975
2) Kubo 1957, Greenwood 1958
3) Butcher 1972

conclusion:

- low conductivity due to lacking diffusive states at ϵ_F

Spectral features of Al_3V: Pseudogaps

Pearson's handbook, no. 139 (DO_{22})
tetragonal unit cell (●): 6 Al, 2 V

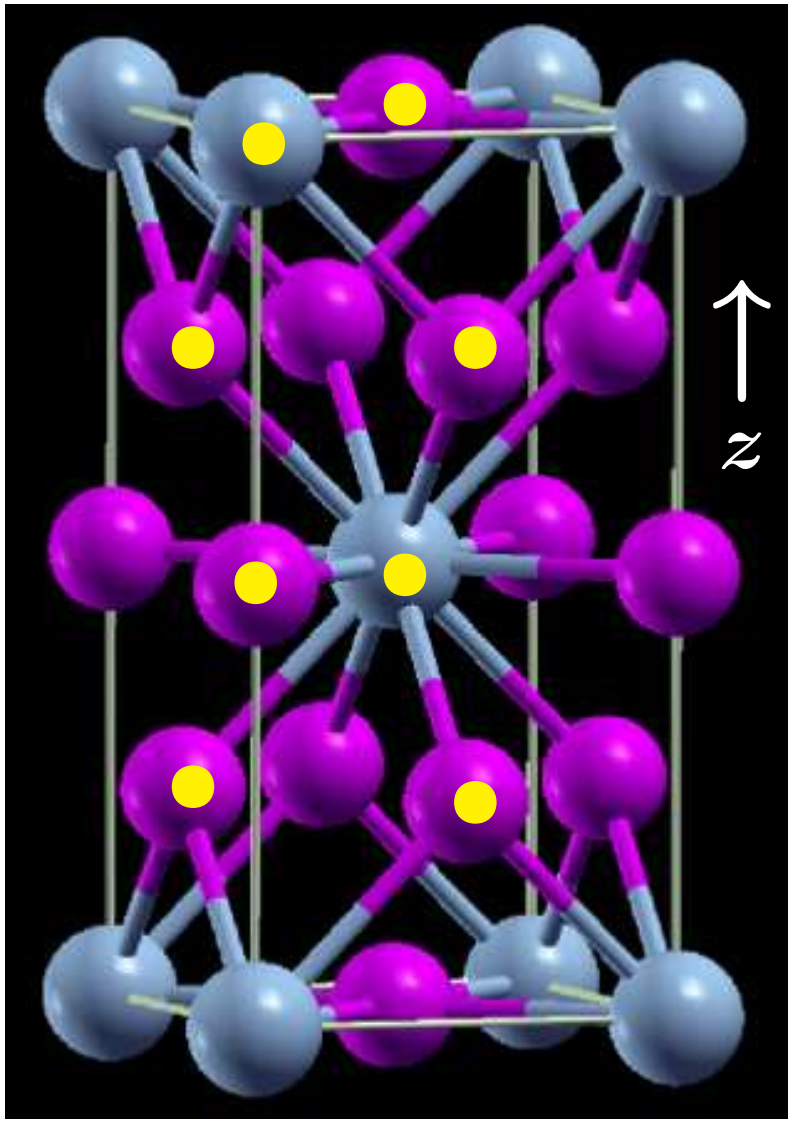

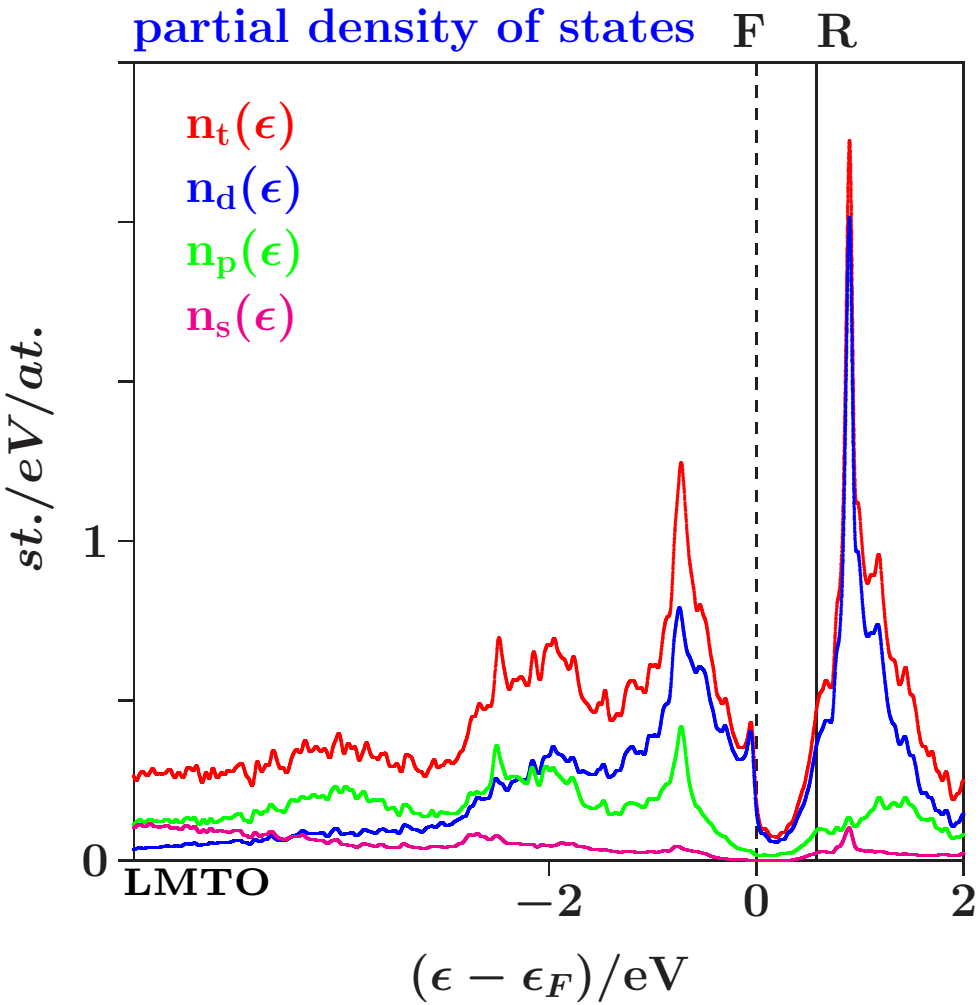

conclusions:

- **sp-DOS: wide, deep pseudogaps centered at ϵ_F**
- **d-DOS: low between ϵ_F and ϵ_R, peak-dip feature at ϵ_F**

Spectral features of Al_3V: Anisotropies

V-Al-V density bridges (↘)
iso-density surface 0.033 e/au^3

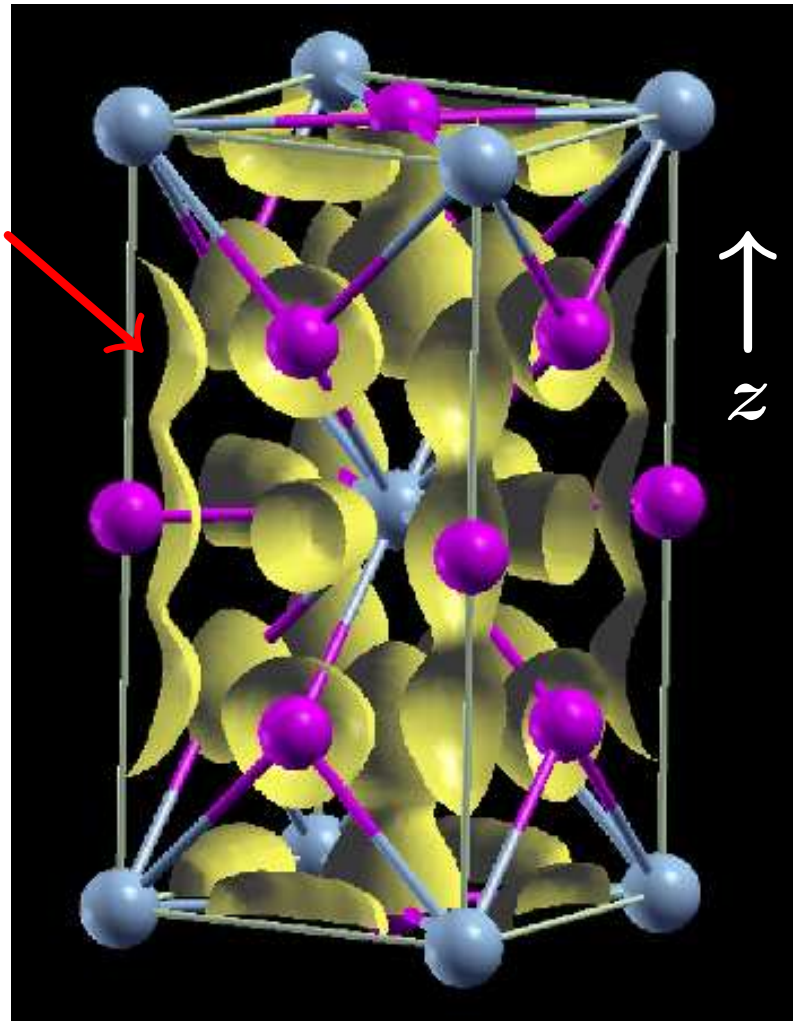

ABINIT

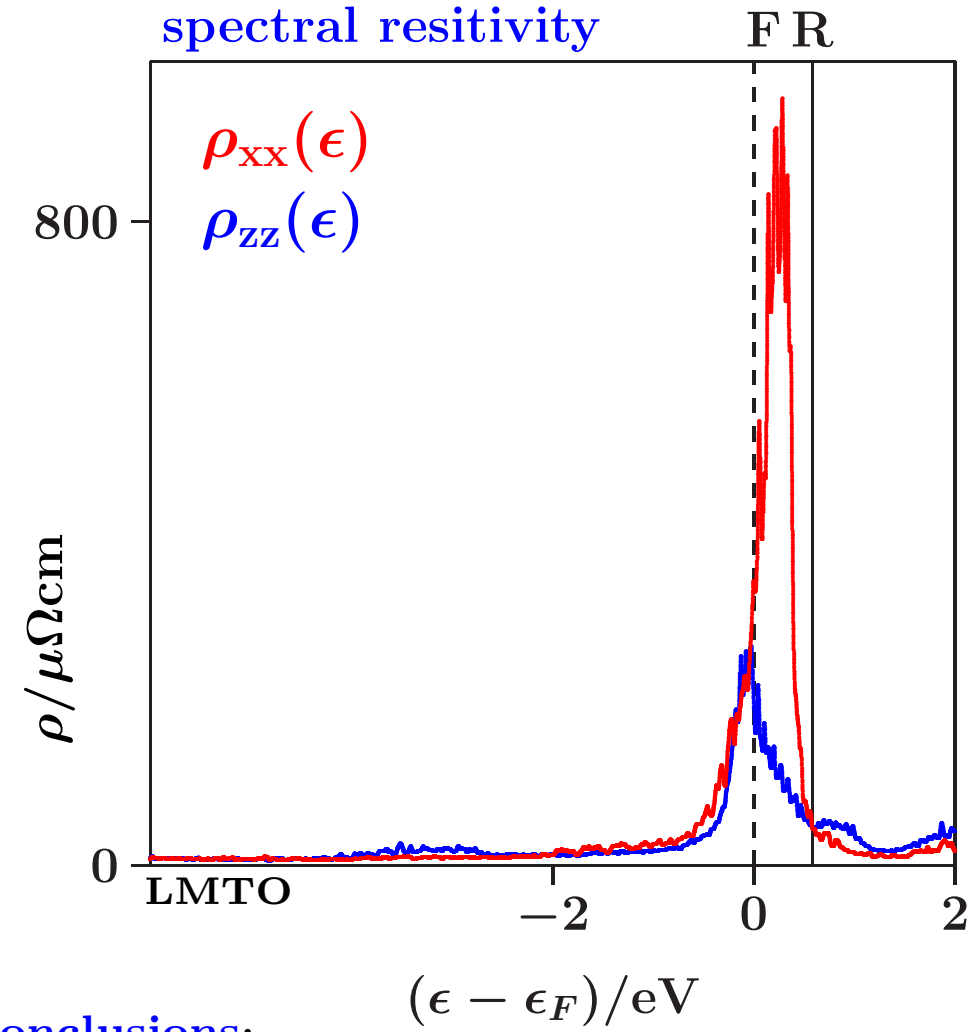

conclusions:

- clearly anisotropic transport between ϵ_F and ϵ_R
- valence density: V-Al-V bridges along z, V-V links along xy

Spectral features of Al_3V: Covalent bonding

bond charges (↘)
on short Al-V bonds,
iso-density surface 0.041 e/au^3

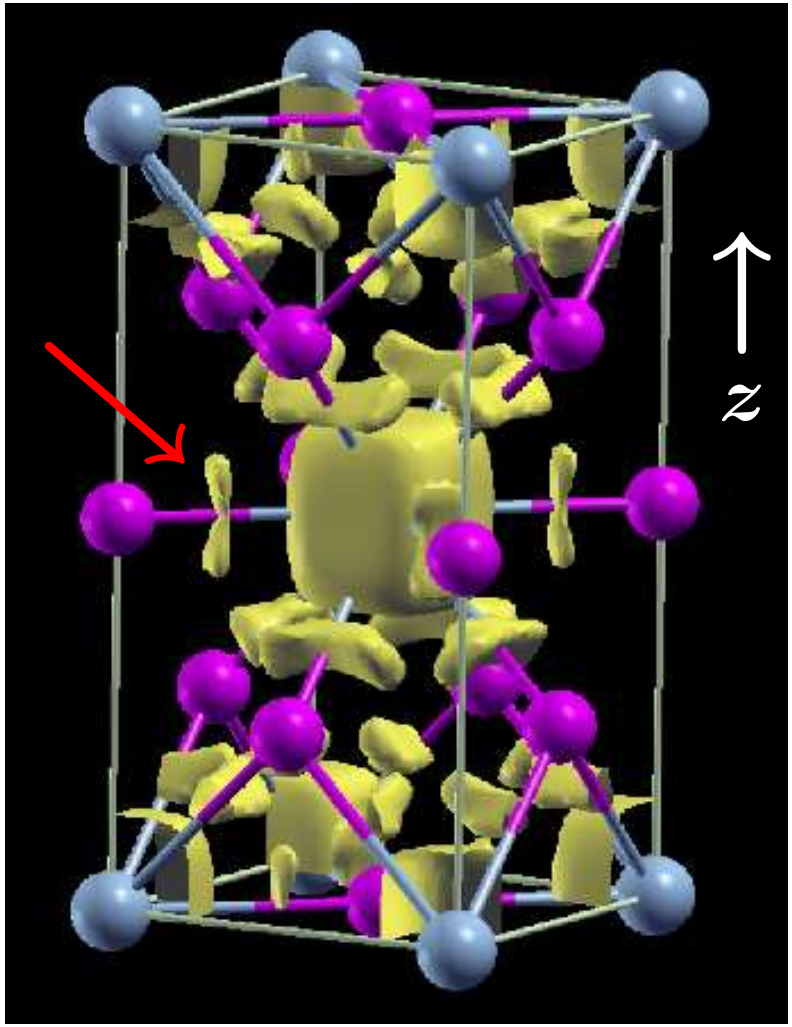

ABINIT

experiment: α-AlMnSi
synchrotron radiation reveals covalent Al-Mn bonding
(Kirihara *et al.* 2000)

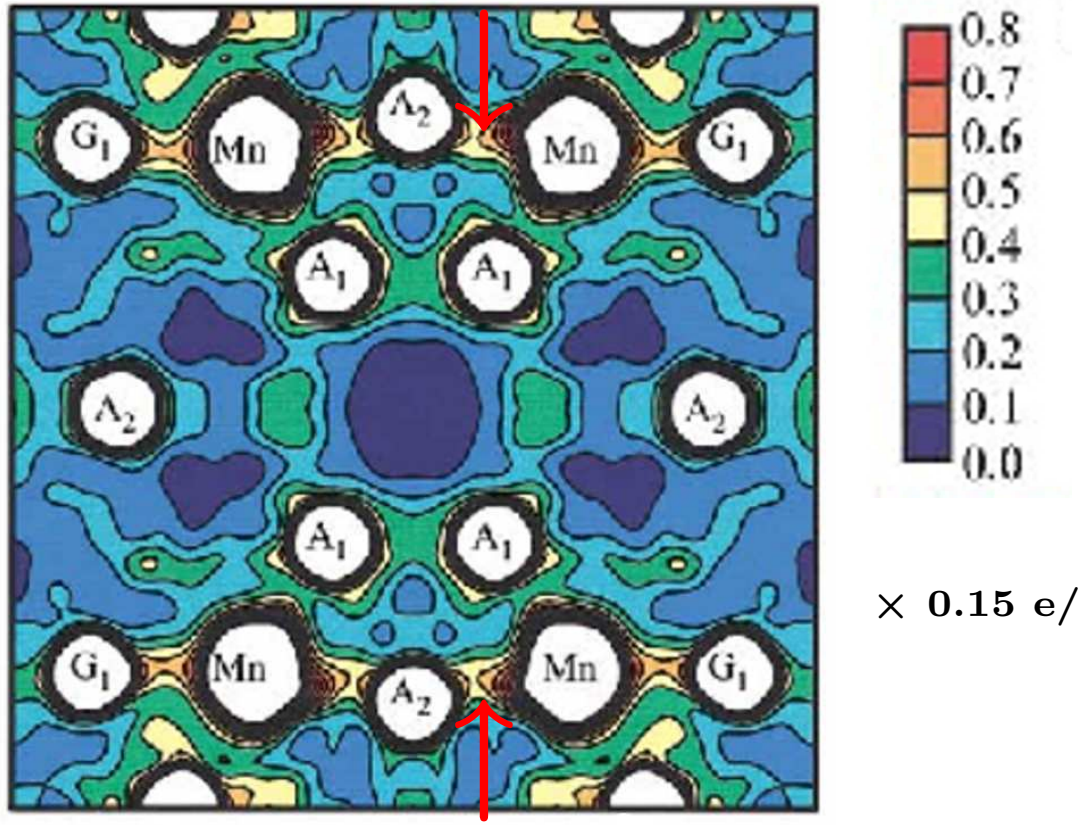

$\times$ 0.15 e/au^3

conclusion:

- covalent bonding between metallic components

1. Basic aspects
2. Electronic properties derived from spectral information

3. Spectral curves are formed by electronic interference

4. Conclusions

Bare effective atoms: The electronic density of states (DOS)

take an atomic sphere (AS) from LMTO, fix the inside potential, remove environment

electronic density of states of the AS:

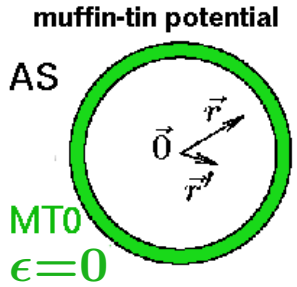

$$n^o(\epsilon) = -\frac{2}{\pi} \overbrace{\int_{AS} d^3\vec{r} \int_{AS} d^3\vec{r}'\, \delta(\vec{r}' - \vec{r})}^{\text{the trace}} \Im G(\vec{r}', \vec{r}, \epsilon)$$

$$= \sum_l n_l^o(\epsilon)$$

AlFe

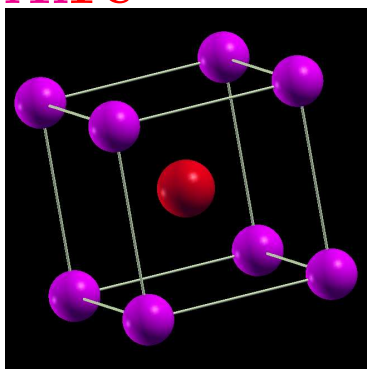

atomic spheres of an AlFe crystal

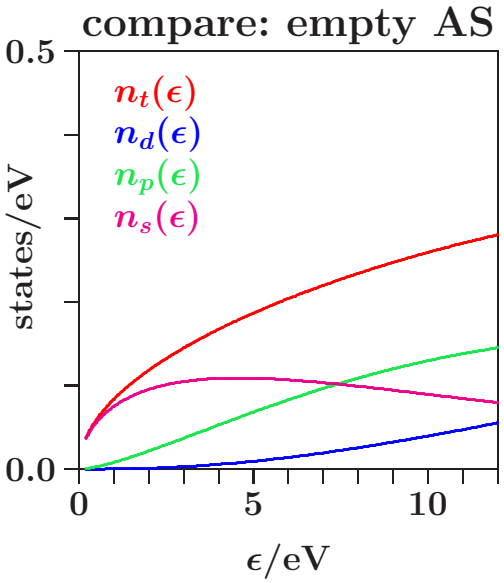

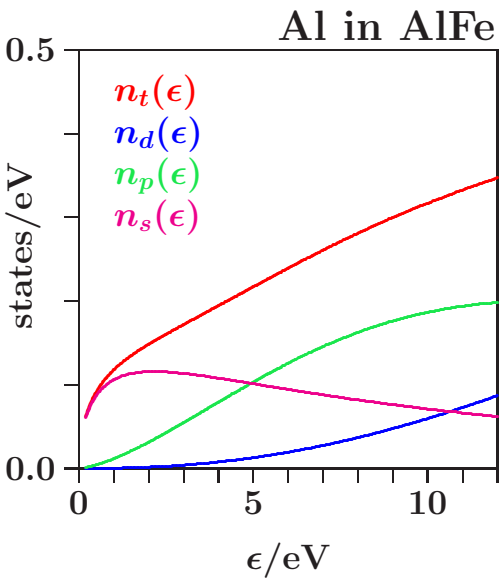

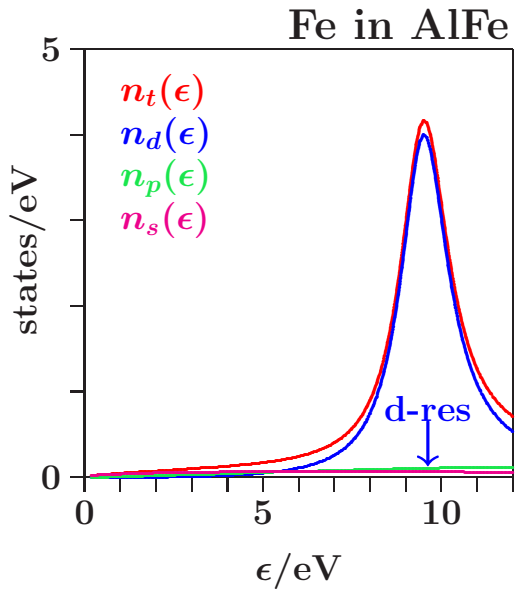

conclusion:

- **the effective atoms: Al is clearly FE-like, TMs contribute virtual bound states**

Bare effective atoms: The scattering phase shifts

scattering amplitudes $f_l(\epsilon)$ and phase shifts $\eta_l(\epsilon)$ of the bare AS:

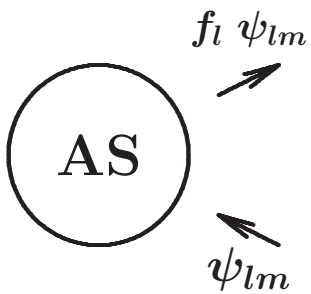

$$f_l(\epsilon) = \frac{1}{2}\left(e^{i2\,\eta_l(\epsilon)} - 1\right)$$

$$\Longrightarrow \quad -1 \quad \text{for} \quad \eta_l \Longrightarrow \frac{\pi}{2}$$

AlFe

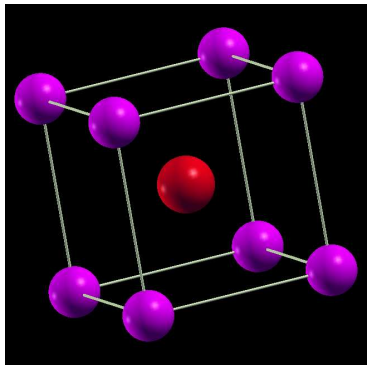

atomic spheres of an AlFe crystal:

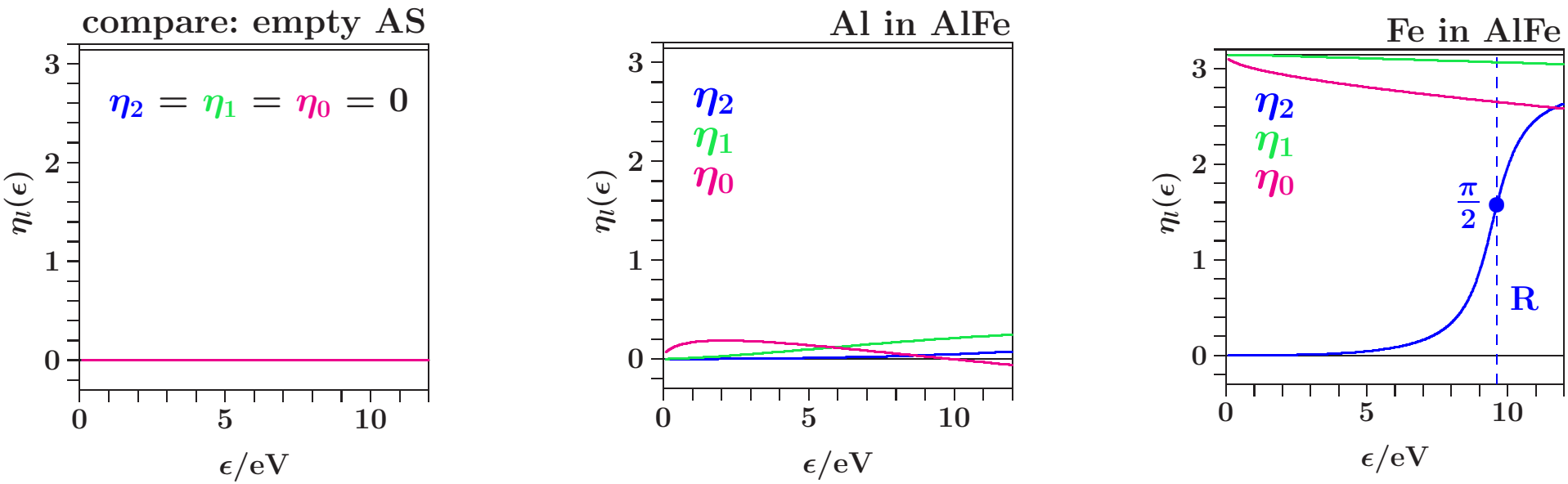

conclusion:

- **scattering by the effective atoms: Al - weak, TMs - strong with fast spectral variation**

Each AS makes a "structure analysis" of its environment

suppose, we know the self-consistent atomic spheres (partial DOS $n^o_{sl}(\epsilon)$, phase shifts η_{sl})

electronic density of states of the ASs including modification by the environment:

$$n_s(\epsilon) = -\frac{2}{\pi} \int_{ASs} d^3\vec{r}\, \Im\, G(\vec{r},\vec{r},\epsilon) = \sum_l n^o_{sl}(\epsilon) \left(1 + \Re \frac{1}{2\,l+1} \sum_{m=-l}^{l} T_{sL,sL}(\epsilon) \right)$$

$\{T_{sL,s'L'}\}$, the scattering-path matrix ($L = l, m$)

$$T_{sL,sL} = e^{i\eta_{sl}} \overbrace{\langle sL| \left(I - PF\right)^{-1} P|sL\rangle}^{\text{multiple scattering of vacuum waves}} e^{i\eta_{sl}}$$

propagation scattering

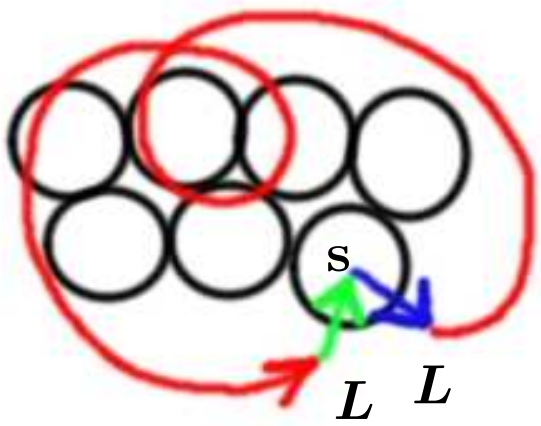

conclusion:

- spectral features arise from the interference of scattering-path contributions

Fano profiles: Interaction line/continuum i.e. fast/slow

simple model: 1 Al and 1 Cu at nearest neighbor distance

How does the Al p-DOS change?

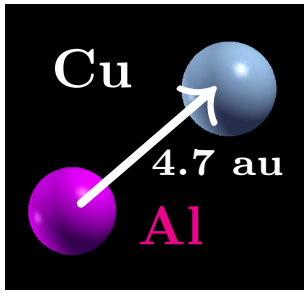

$$n_{Al,1}(\epsilon) = n^o_{Al,1}(\epsilon)(1 + \Re \underbrace{\frac{1}{3}\sum_{m=-1}^{1} T_{Al,1m;Al,1m}(\epsilon)}_{\equiv T_{Al,1;Al,1}})$$

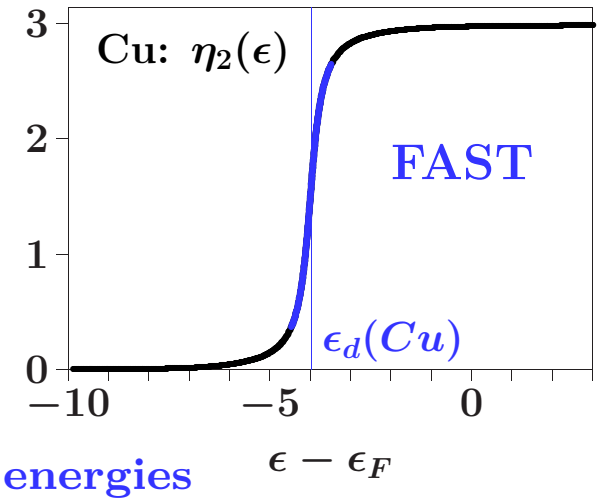

a resonant nearest neighbor moves spectral weight to lower energies

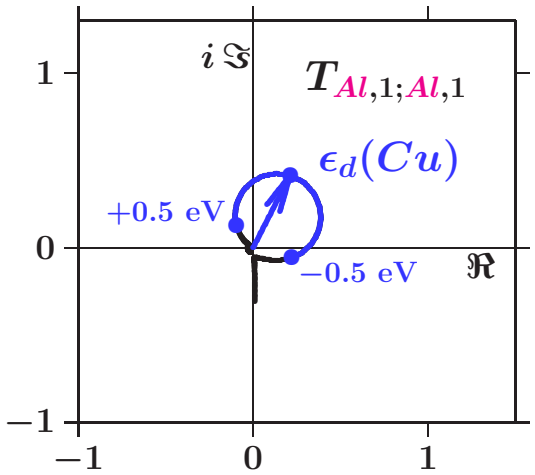

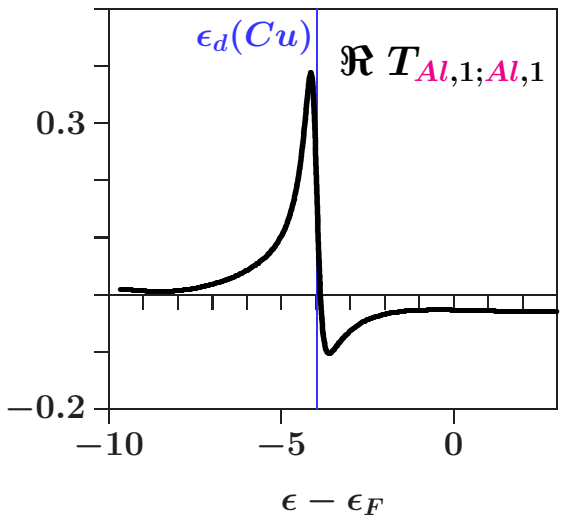

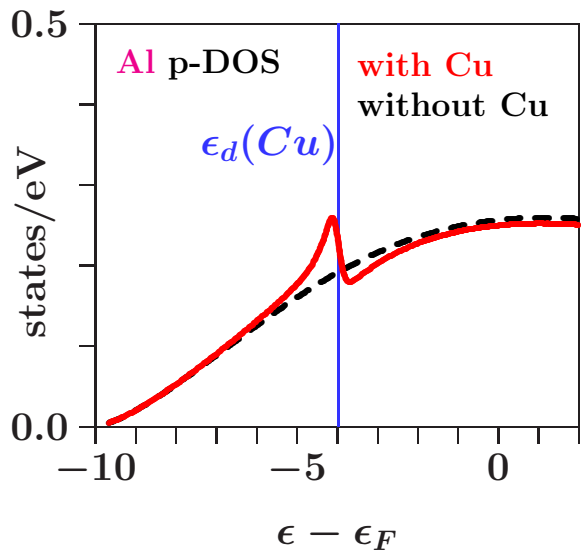

conclusion:

- enhanced Al p-DOS below the d-TM resonance

i-AlCuFe-(1/1): Stabilizing Fano profile at the Fermi level

A crystalline approximant of the icosahedral Al-Cu-Fe quasicrystal (Cockayne 1993)

cubic cell: 128 atoms = 80 Al + 32 Cu + 16 Fe

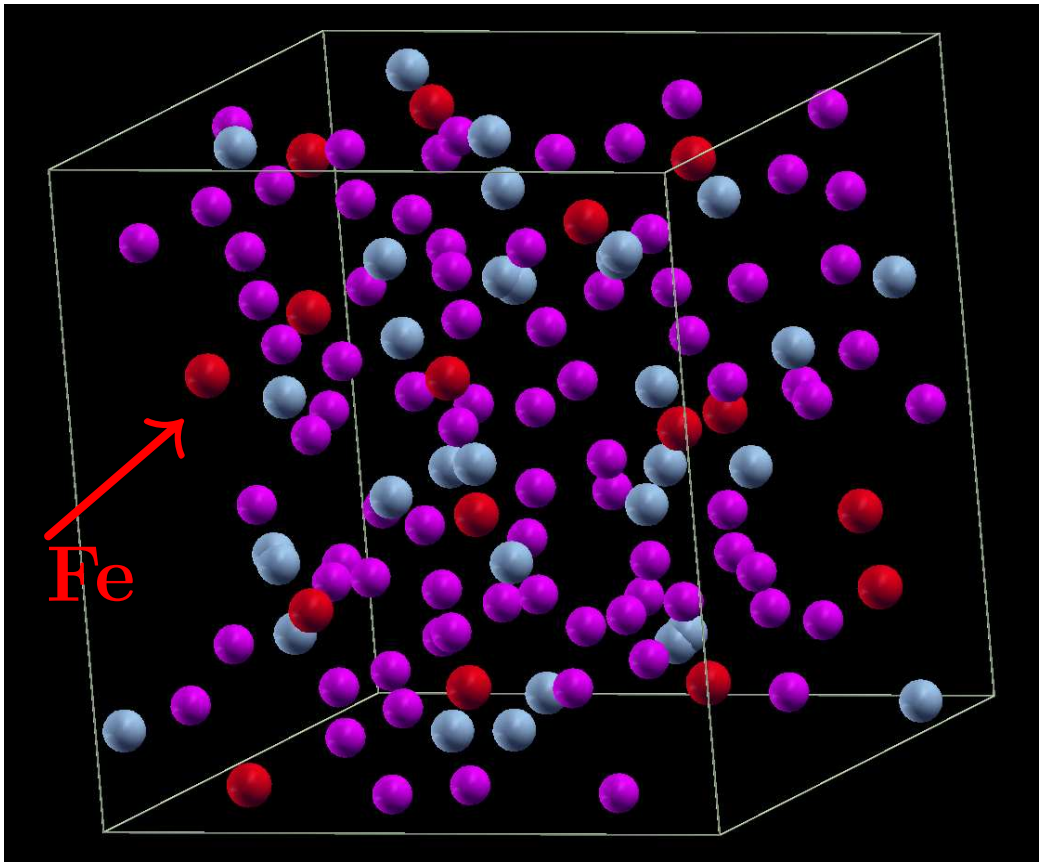

Fano effect at the Fermi energy,

fast spectral variation due to multiple scattering in the Fe sublattice

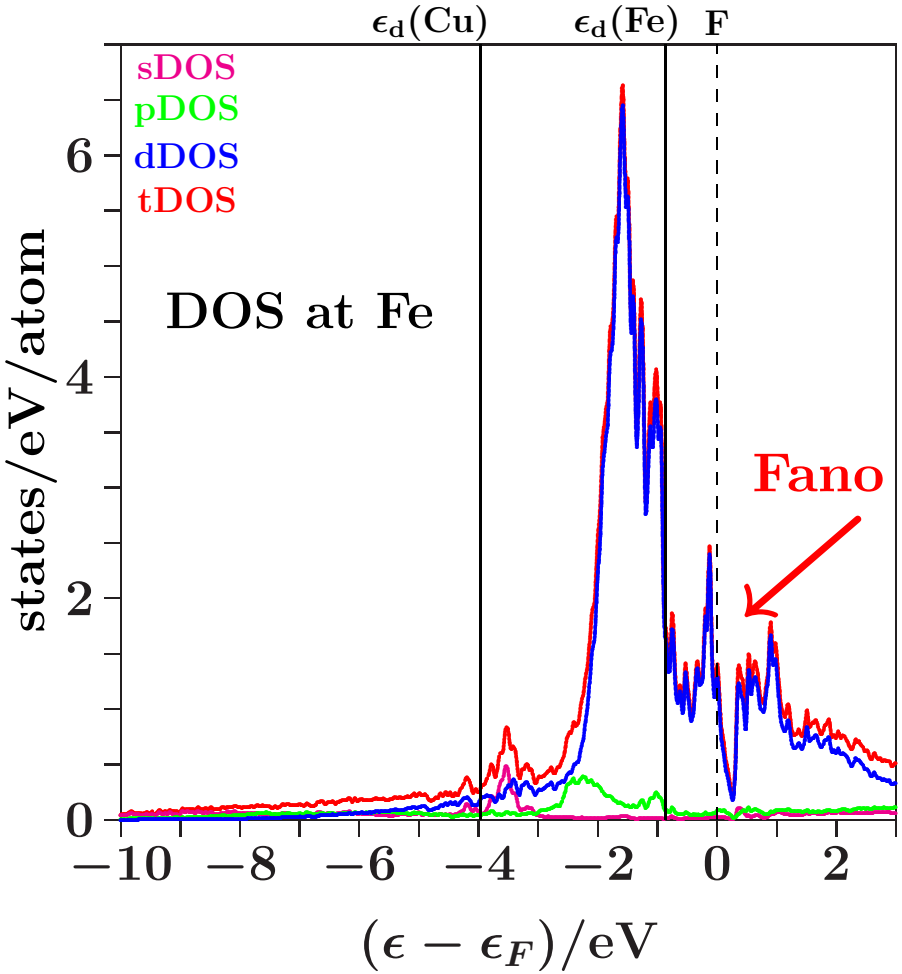

conclusion:

- the fast process can also arise from a sublattice

Weak scatterers: Influence of the medium-range order

one atom (e.g.Na) couples to

a distant cluster ($\Rightarrow$ asymtotic expansion)
of weak scatterers ($\Rightarrow$ single scattering)

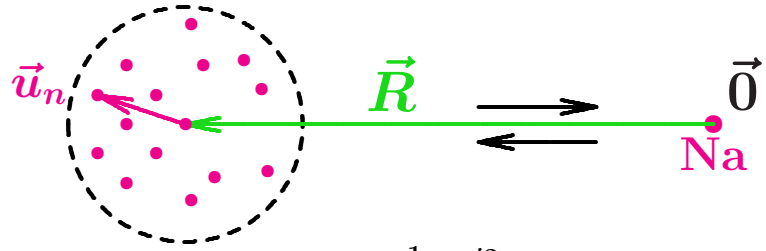

weak scatterers, $f_l = \frac{1}{2}\left(e^{i2\eta_l} - 1\right)$

confine to the sDOS of Na

$$n_{Na,0} = n^o_{Na,0}\left(1 + \Re\, T_{Na,0;Na,0}\right)$$

$$T_{Na,0;Na,0} \approx e^{i\eta_o}\frac{e^{ikR}}{ikR}\underbrace{\sum_{n}^{\text{scatterers}} e^{i2k\hat{\vec{R}}\vec{u}_n}}_{\substack{\text{structure amplitude F(-1)}\\ \text{for}\\ \text{backscattering}}}\underbrace{\sum_{l}(2l+1)f_l(-1)^l}_{\substack{\text{scattering amplitude}\\ \text{for}\\ \text{backscattering}}}\frac{e^{ikR}}{ikR}e^{i\eta_o}$$

conclusion:

- strong backscattering if all exponentials in the structure amplitude are "in phase"

Crystals: Friedel-spaced lattice planes

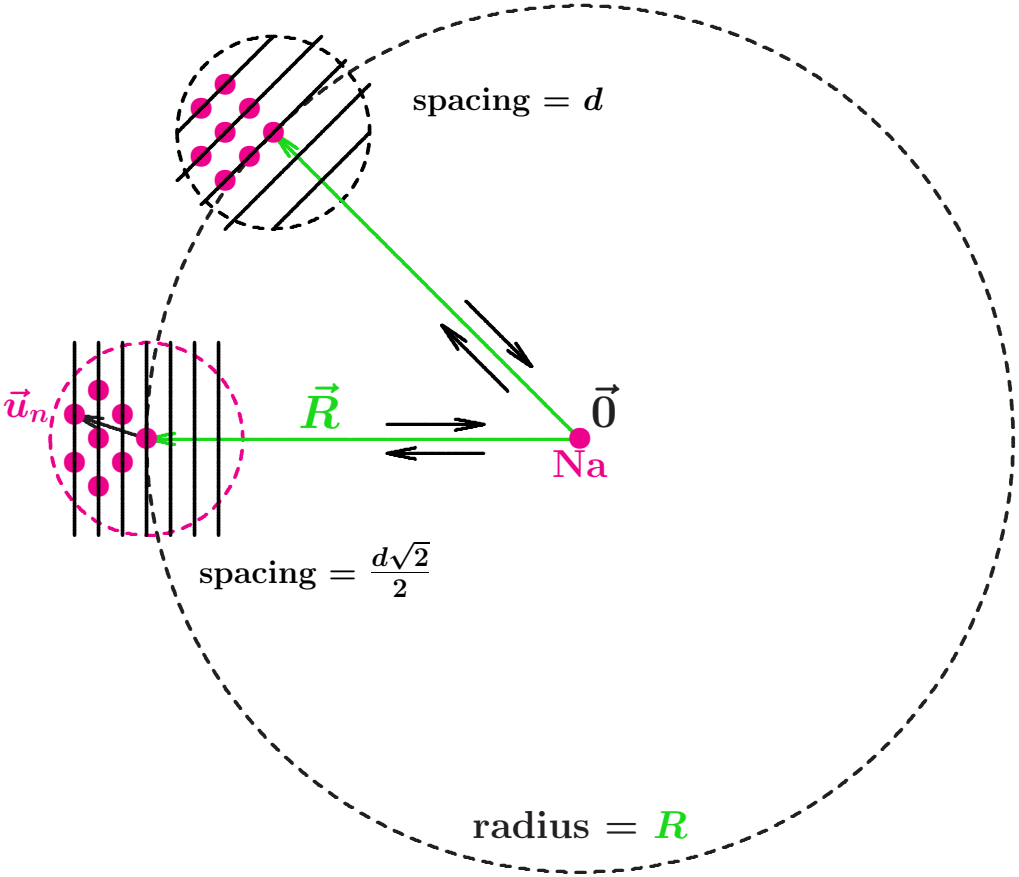

The structure amplitude,

$$F(-1) = \sum_{n}^{\text{scatterer}} e^{i2k\hat{\vec{R}}\vec{u}_n},$$

will be large if

- the cluster atoms are densely arranged on planes perpendicular to $\hat{\vec{R}}$
- the plane spacing is

  $$2\pi/2k$$

  which is a Bragg condition.

conclusions:

- interference-supported spectral structures even deep in the valence band
- electrons at ϵ_F support plane spacings $\approx 2\pi/2k_F$ (Friedel wave length)
- enhanced electronic influence due to nesting of Bragg reflections (e.g. fcc-type reciprocal lattices, bcc-type real space)

Liquid + amorphous phases: Friedel-spaced neighbor shells

liquid/amorphous *sp* phases, for simplicity only s waves considered

$$n_0(\epsilon) \approx n_0^o(\epsilon)\left\{1 + \frac{2\pi\mathcal{N}_{at}\,sin(\eta_0)}{k^3}\left(\overbrace{cos(3\eta_0)}^{\text{inward reflection by a homogeneous medium}} + \overbrace{\int_0^\infty d(2kr)\,(g(r)-1)\,sin(2kr+3\eta_0)}^{\text{inward reflection by the neighbor shell sequence}}\right)\right\}$$

compare with the structure factor

$$S(q) - 1 = \frac{4\pi\mathcal{N}_{at}}{q^3}\int_0^\infty d(qr)\,qr\,(g(r)-1)\,sin(qr)$$

constructive interference if $g(r)-1$ and $sin(2k\,r)$ oscillate with the same radial period

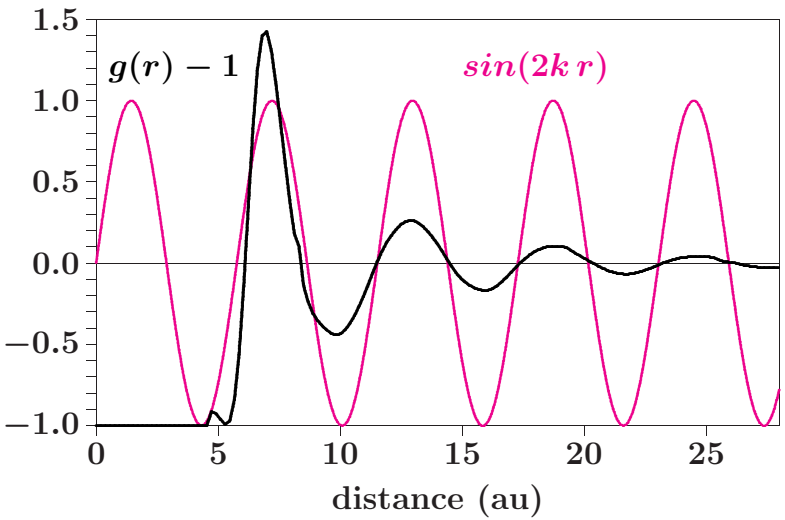

conclusion:

if radial period = Friedel wavelength $= \frac{2\pi}{2k_F}$

then structure fitted to electrons at ϵ_F and main diffraction peak K_p close to $2k_F$

Weak interference: Liquid Na at 378 K

partial DOS (LMTO, **single backscattering by 65 000 neighbors**)

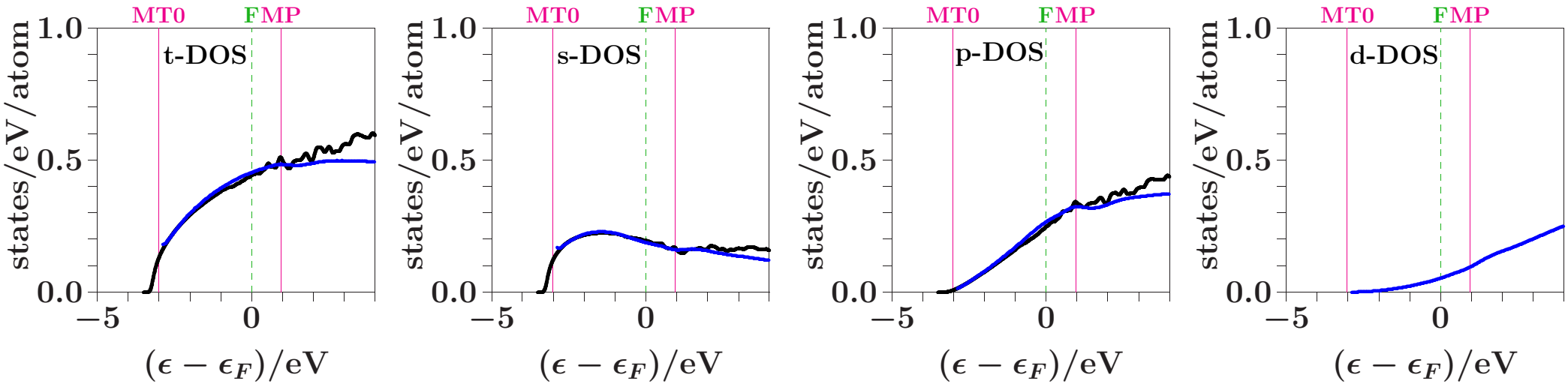

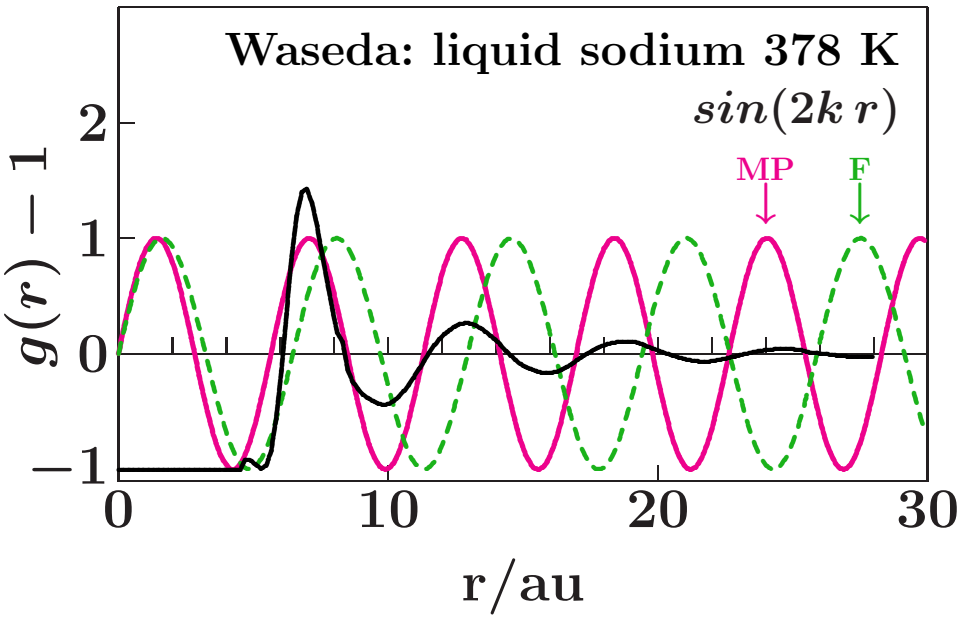

onset energy of diffraction influence:

$$\text{MP} = (K_p/2)^2 \text{ ryd above MT0}$$

conclusions:

- neighbor shell spacing **not perfectly** fitted to interference at ϵ_F
- interference **above ϵ_F** weakened due to thermal shell broadening
- no notable multiple scattering

Weak interference below ϵ_F: Na-bcc

partial DOS (LMTO, **single backscattering by 65 000 neighbors**)

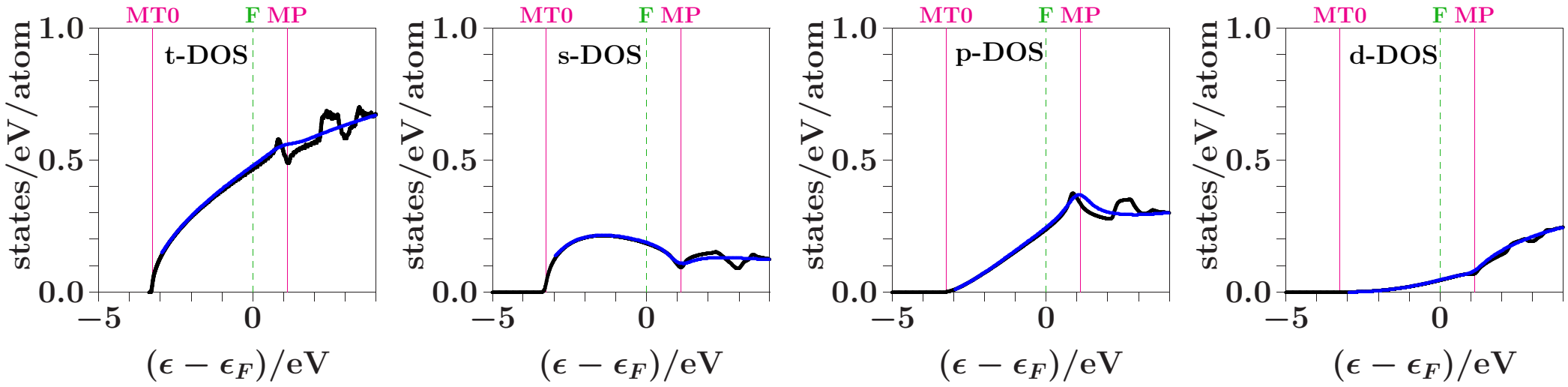

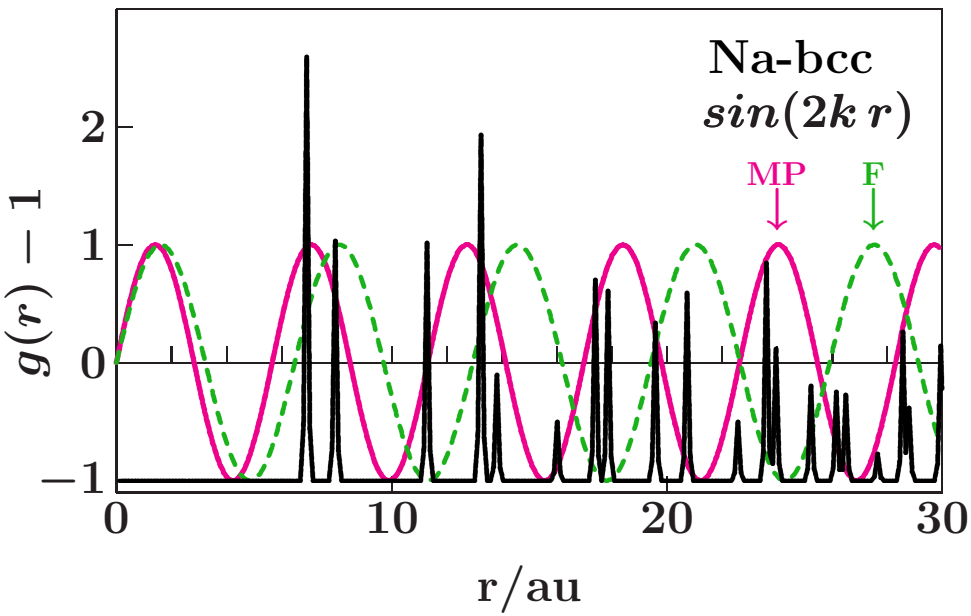

onset energy of diffraction influence:

$$\text{MP} = (K_p/2)^2 \text{ ryd above MT0}$$

conclusions:

- in the occupied valence band:
  weak interference,
  single backscattering is sufficient
- high ductility expected

Covalent bonding and medium-range interference: Si-dia

diamond lattice = 2 × fcc

centered tetrahedra in 4 of 8 octants

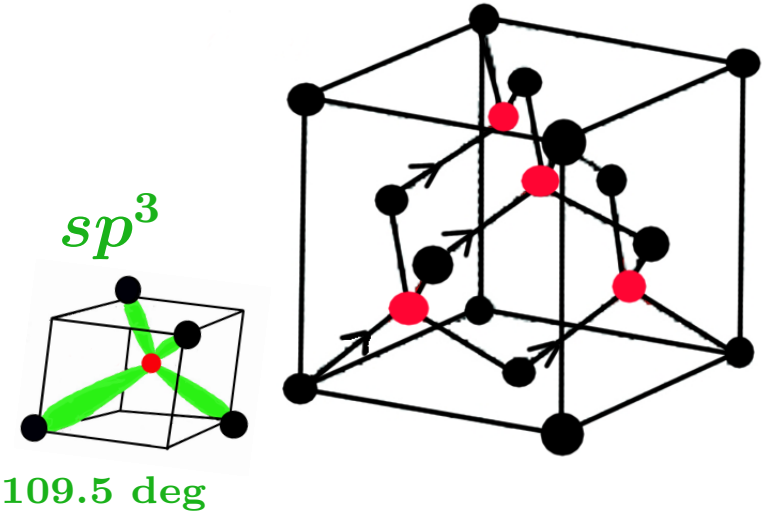

structure factor of neighbor shells

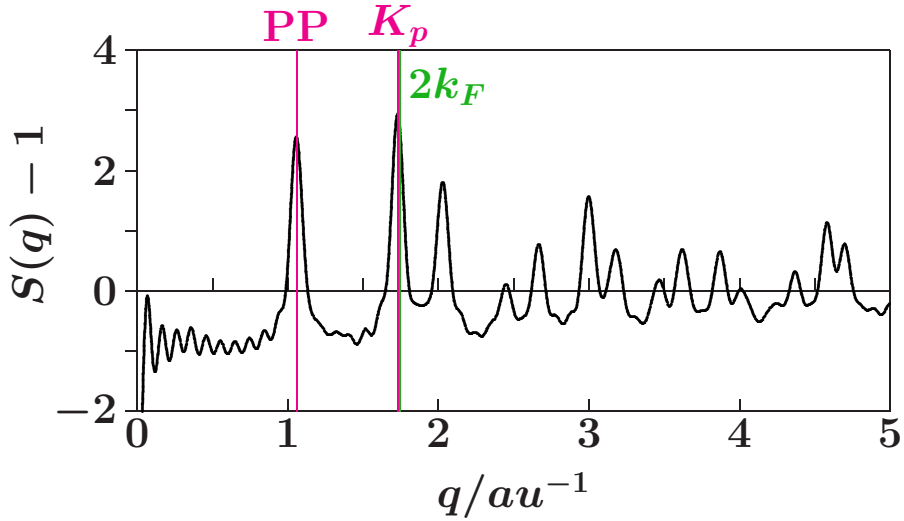

Diamond lattice: Origin of the prepeak

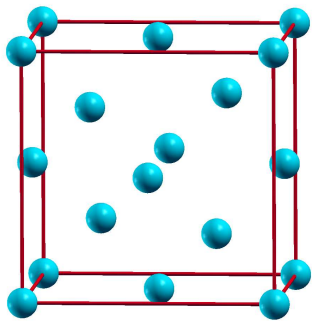

dia

incomplete tessellation

+

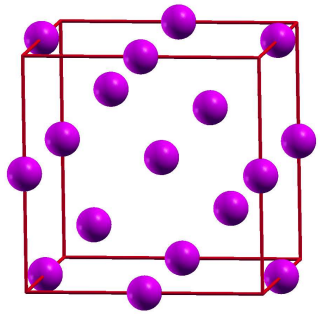

dia - the holes

incomplete tessellation

=

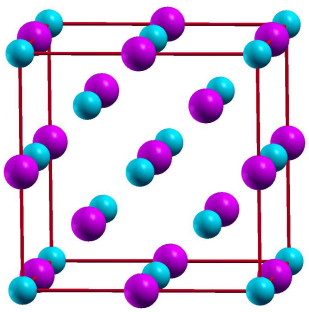

bcc

complete Voronoi tessellation

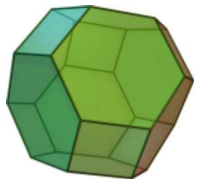

F14 V24 E36

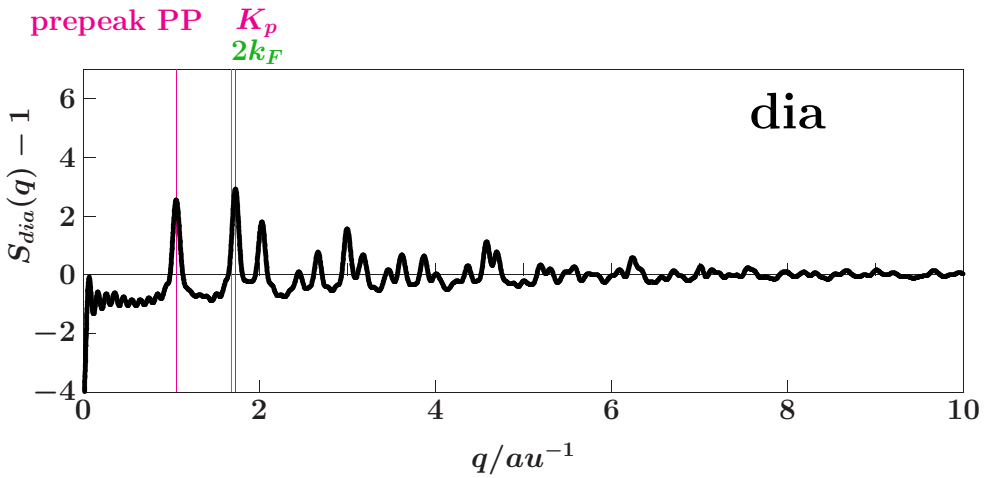

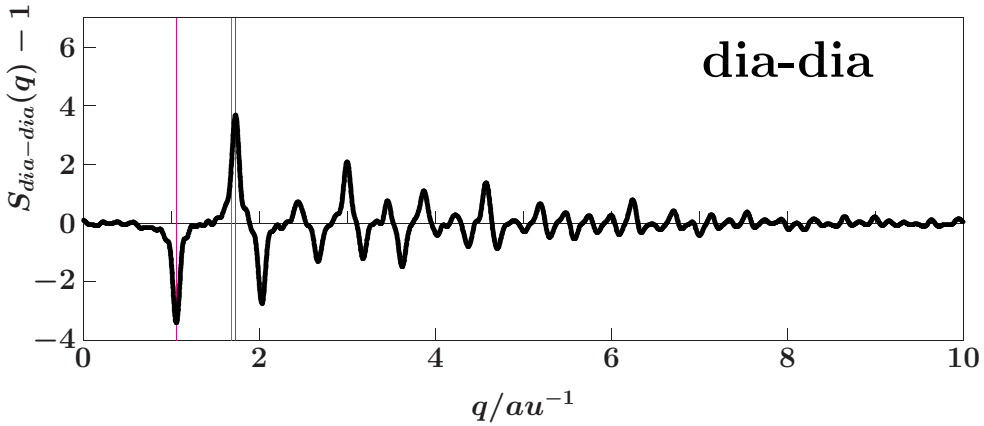

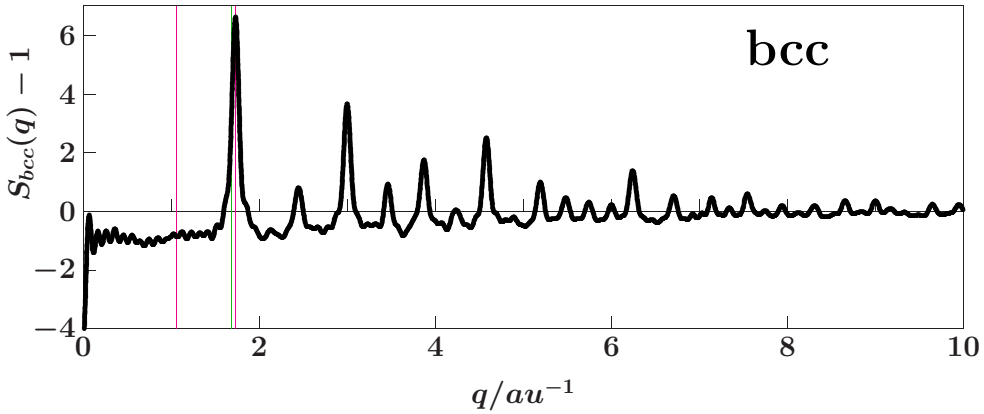

Covalent bonding and medium-range interference: Si-dia

diamond lattice = 2 × fcc

centered tetrahedra in 4 of 8 octants

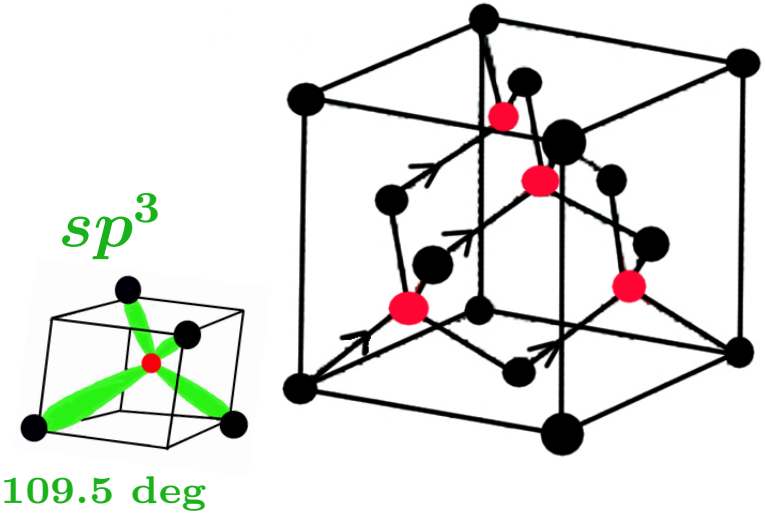

structure factor of neighbor shells

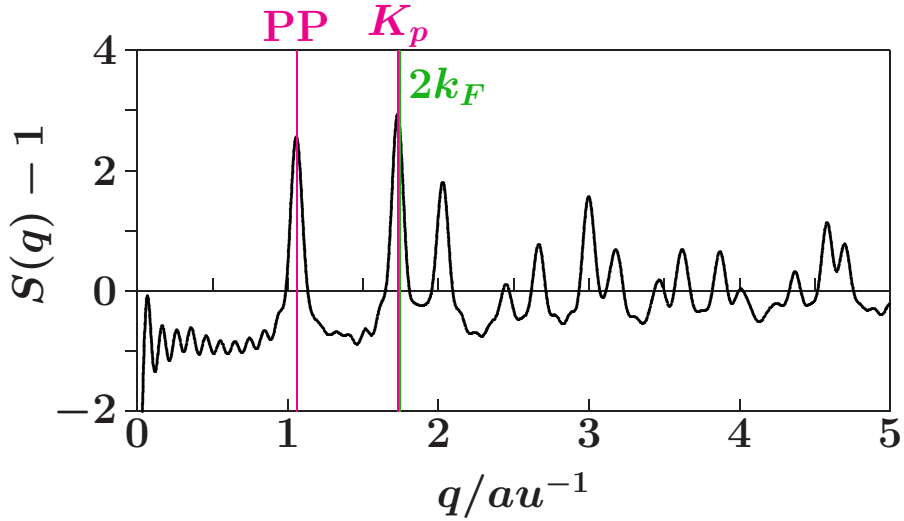

density of states

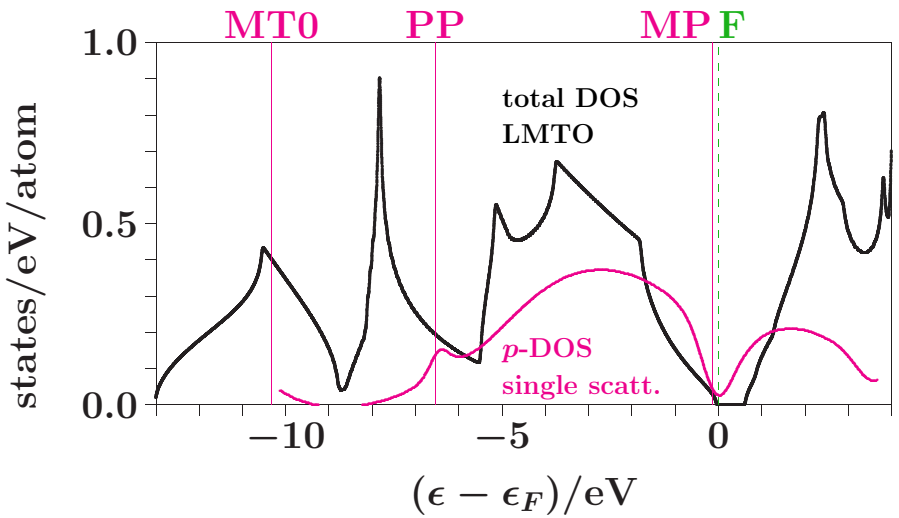

conclusions:

- **Si network**: covalent bonding by means of local sp^3 hybrides, gap at ϵ_F
- **Si neighbor-shell sequence**: structure factor has main diffraction peak K_p at $2k_F$, ϵ_F in ryd above MT0
- **single scattering p-DOS**: 65 000 neighbors, deep pseudogap at ϵ_F

General Conclusions

Spectral curves are formed by the
interference of scattering-path contributions.

Stabilizing processes shift occupied electron states to lower energies.

Peculiar temperature dependence results from spectral features close to the
thermal energy scale.

Nearly-free electron arguments
are valid if main diffraction peaks are nested close to $2k_F$.
However,
there are no reliable rules for matching the energy scales.